Available online at www.sciencedirect.com
SCIENCE DIRECT®
Journal of Magnetic Resonance 163 (2003) 288–299
JMR Journal of Magnetic Resonance
www.elsevier.com/locate/jmr

Dipolar Waves as NMR maps of helices in proteins

Michael F. Mesleh and Stanley J. Opella*

Department of Chemistry and Biochemistry, University of California, San Diego, La Jolla, CA 92093, USA

Received 17 January 2003; revised 21 March 2003

Abstract

Dipolar Waves describe the periodic variation in the magnitudes of dipolar couplings in the backbone of a protein as a function of residue number. They provide a direct link between experimental measurements of dipolar couplings in aligned samples and the periodicity inherent in regular secondary structure elements. It is possible to identify the residues in a helix and the type of helix, deviations from ideality, and to orient the helices relative to an external axis in completely aligned samples and relative to each other in a common frame in weakly aligned samples with Dipolar Waves. They provide a tool for accurately describing helices and a step towards high throughput structure determination of proteins.

1. Introduction

Dipolar Waves describe the periodic variation in the magnitudes of dipolar couplings in the backbone of a protein as a function of residue number [1]. Unaveraged and residual dipolar couplings are measured with NMR experiments on completely and weakly aligned samples, respectively. The sinusoidal oscillation of the ^{1}H–^{15}N dipolar couplings from backbone sites of the residues in helices is a particularly clear-cut example of the mapping of protein structure onto NMR spectral parameters by the anisotropy of the nuclear spin interactions in aligned samples [2]. The characteristic 3.6 residues per turn periodicity of α-helices results in Dipolar Waves with the same period. The magnitudes and average values of the dipolar couplings fit to a sinusoid with this period characterize the absolute orientations of helices in the laboratory frame in completely aligned samples, and the relative orientations of helices in a common molecular frame in weakly aligned samples. In this article we describe the basic properties of Dipolar Waves for 3_{10} helices and π helices, and provide a more detailed analysis of the application of Dipolar Waves to α-helices than in our initial reports [1,2]. Similar analyses are feasible for β-sheet [3] as well as other types of periodic structures found in proteins, nucleic acids, or other polymers.

Empirical correlations have been found between the 3.6 residues per turn periodicity of α-helices and measurements in several other magnetic resonance experiments. The site-directed spin labeling EPR experiments developed by Hubbell and coworkers [4] have made use of this periodicity to examine the structures of peptides and proteins both in lipid environments and in solution [5]. This periodicity has also been used to calibrate distances between spin-labels in peptides based on the 1.5 Å rise per turn of α-helices [6]. Studies of the $^{1}H^{\alpha}$ NMR resonances of residues in α-helices have demonstrated that there are systematic chemical shift changes [7–10] as well as periodicities in the secondary chemical shifts [11–13]. All of these measurements have been used to characterize the local structure and deformations of helices, interpreting them as changes in the local environment and distortions of hydrogen bonding geometry. In contrast, Dipolar Waves enable the simultaneous identification of the residues in a helix, type of helix, and deviations from ideality based solely on the intrinsic periodicity of the secondary structure. Moreover, this can generally be accomplished with the results of one experiment on a uniformly ^{15}N-labeled sample with an unmodified sequence obtained by expression in bacteria.

Along with the overall rotational correlation time and the resonance assignment strategy, sample alignment is an essential component in the design and implementation

* Corresponding author. Fax: 1-858-822-4821.
E-mail address: sopella@ucsd.edu (S.J. Opella).

1090-7807/$ - see front matter © 2003 Elsevier Science (USA). All rights reserved.
doi:10.1016/S1090-7807(03)00119-8

of NMR structural studies of proteins [2]. Samples can generally be prepared with no, weak, or complete alignment of the protein molecules. In the past, the vast majority of NMR studies of proteins were performed on isotropic samples without molecular alignment; however, this situation has changed, and aligned samples are now widely used in both solid-state NMR [14], as originally demonstrated with single crystals of small molecules [15] and uniaxially aligned polymer fibers [16], and in solution NMR [18], where there is a long history of applications to small molecules aligned in liquid crystals [17] and through diamagnetic anisotropy [19]. Soluble proteins can be weakly aligned in a variety of media for solution NMR studies. Applications to membrane proteins in bilayers are of particular interest [20], since the polypeptides are immobilized by their interactions with lipids and can be completely aligned between glass plates to an extent that rivals that of single crystals [21]. It is also possible to weakly align membrane proteins in micelles for solution NMR studies by the addition of lanthanide ions [22,23] or their incorporation into compressed (or stretched) gels [24–26]. Applications of Dipolar Waves to membrane proteins in weakly aligned micelles and completely aligned bilayers will be described separately.

2. Materials and methods

The template helices utilized in the spectral simulations were generated using the Biopolymer module of Insight II (Accelrys, San Diego, CA) running on a Silicon Graphics O_2 computer (Mountain View, CA) and analyzed using the program HELANAL [27]. Standard bond lengths and angles [28] were used to build model α-helices ($\Phi = -65°$, $\Psi = -40°$), π-helices ($\Phi = -57°$, $\Psi = -70°$), and 3_{10}-helices ($\Phi = -49°$, $\Psi = -26°$) with their long axes aligned with the screen z-axis. Torsion angles corresponding to a canonical curved helix were taken from the model proposed by Zhou et al. [29], where the values of the dihedral angles on one "hydrophobic" face of the helix ($\Phi_{i+1} = -59°$, $\Psi_i = -44°$) differ from those on the other "hydrophilic" face ($\Phi_{i+1} = -66°$, $\Psi_i = -41°$). More highly curved helices were built with the values ($\Phi_{i+1} = -67°$, $\Psi_i = -44°$) on one face and ($\Phi_{i+1} = -63°$, $\Psi_i = -40°$) on the other. The magnitudes of heteronuclear dipolar couplings were simulated using the program SIMSPEC [30], whose input consists of a PDB file containing the three-dimensional coordinates of the template, values for the magnitude of the axial component of the alignment tensor (A_a), rhombicity (R), and rotations to be applied about the x, y, and z axes. The output from the program is a list of the orientation-dependent ^1H–^{15}N heteronuclear dipolar couplings for each backbone amide site in the protein using the screen x, y, and z cordinate axes to define the alignment frame of reference. The values of residual dipolar couplings (RDCs) are calculated using Eq. (1):

$$D_{\mathrm{RDC}} = \frac{\mu_0 \hbar \gamma_{\mathrm{H}} \gamma_{\mathrm{N}}}{8\pi^2 r^3} A_a \left\{ (3\cos^2\theta - 1) + \frac{3}{2} R \sin^2\theta \cos 2\phi \right\}, \quad (1)$$

where μ_0 is the permittivity of free space; $\hbar$ is Planck's constant; γ_H and γ_N are the gyromagnetic ratios of ^1H and ^{15}N, respectively; and θ and ϕ are the spherical polar coordinates that describe the orientation of the ^1H–^{15}N bond axis in the alignment frame. In these calculations, r, the NH bond length is taken to be 1.04 Å, which has been empirically observed to optimize the fit to experimentally measured values. In the special case of a sample that is completely uniaxially aligned parallel to the direction of the applied magnetic field (z), the magnitude of A_a is equal to 1 and R is zero.

All of the experimental datasets of ^1H–^{15}N RDCs analyzed in this article were obtained from the BioMagRes database (Madison, WI) [31]. The corresponding structures of these proteins were obtained from the Protein Databank (Research Collaboratory for Structural Bioinformatics, NJ, SD, MD) [32]. The proteins were chosen because of their relatively high (53–70%) helix content, and include: G-α Interacting Protein [33] (MR1597 and PDB 1CMZ); Ribosomal Protein S4δ41 [34] (MR1292 and PDB 1C06); Rat apo-S100B [35] (MR790 and PDB 1B4C); Phosphoryl Transfer Complex Hpr [36] (MR7366 and PDB 3EZA); DnaB helicase [37] (MR4297 and PDB 1JWE); and Human Barrier to Autointegration Factor [38] (MR7116 and PDB 2EZX). The coordinates for the average solution NMR structure and the 1.40 Å resolution crystal structure of cytochrome b_{562} were obtained from the PDB from accession codes 1QPU [39] and 256B [40], respectively.

All of the plotting and fitting routines were implemented in MATLAB Version 6 (MathWorks) in a LINUX operating system on a PC-based computer. The fitting of sinusoids to the experimental data is performed in two ways using the standard unconstrained non-linear minimization procedure provided with MATLAB. First, the amplitude and average value of the sinusoid are fitted to the largest and smallest values of the dipolar couplings measured for residues in a helix so that only the phase of a sinusoid with a periodicity of 3.6 is a free parameter. A second fitting algorithm, which allows both the amplitude and average value of the sinusoid to vary with both quadratic and linear terms ($ax^2 + bx + c$) along the helix with the phase also fit to the data, results in good fits to data from helices with curvature or other deviations from ideal helix geometry. In this case, the starting value in the fitting routine for the amplitude is taken as the difference between the largest and smallest values across the helix, and the average represents all of these values. Because this involves the use of seven

fitting parameters, this type of analysis is only meaningful when the number of measurements for a helix exceeds this number.

The residues in an individual helix are identified on the basis of the periodicity of the oscillations of the dipolar couplings of their amide N–H bonds. A sliding window of four residues is applied to the entire sequence, and a score in calculated as the fit parameter for the best-fitted ideal sinusoid with a periodicity of 3.6 residues per turn for each position in the polypeptide. The score for the four-residue sliding window function is assigned to the middle of the window so that the effect of a deviation is centered at its position. In addition to the fit to an ideal sinusoid, the absolute phase of the fit is monitored to ensure that fits for consecutive windows are consistent with a single sinusoid. Fitting of Eq. (2) to the sinusoid yields average helix tilts, and is done with values of D_a (defined as the conglomerate of all the physical constants in Eq. (1) for an amide ^1H–^{15}N bond) and R estimated using the powder-type histogram method [41] and validated by comparison to the values obtained using MODULE [42] with the average solution NMR structure of the protein. In the calculations of helix orientations, only θ_{av}, ϕ_{av}, and ρ_0 are allowed to vary from arbitrary starting values for both θ_{av} and ϕ_{av}, and 0° for ρ_0, while the values for the magnitude and rhombicity of the alignment tensor are held constant. Hydrogen atoms were added to the amide sites in the crystal structures and the orientations of the helices were visualized using MOLMOL [43]. The orientations of the helix axes are determined using the algorithm of Christopher et al. [44] from coordinates that are rotated so that the x, y, and z axes of the alignment tensor are coincident with the screen x, y, and z axes.

3. Results and discussion

The simulation and fitting of dipolar couplings to simple sinusoids relies on the periodicity inherent in the structures of helices being mapped into the spectral parameters measured in NMR experiments on aligned samples. There is a unique mapping of structure to the spectra, which enables spectra to be calculated from structural models [30,45,46], and provide distinctive spectral signatures of periodic secondary structures such as helices and sheets, including PISA Wheels [47,48], PISA Pies [49], and Dipolar Waves [1,2]. Indeed, the frequency of the sine wave that fits the oscillations of the dipolar couplings as a function of residue number is diagnostic of the period for a single turn of each of the three types of helices found in proteins [28]: 3.6 residues per turn for α-helices, 3 residues per turn for 3_{10} helices, and 4.4 residues per turn for π-helices. Similarly, β-sheets have repeats of between 2.0 residues and 2.3 residues [50], although in this case an analogous implementation is complicated by the difficulty in defining a linear axis. The spectral simulations in Fig. 1 compare the principal features of the mapping of the three types of helical structures found in proteins onto the chemical shift and heteronuclear dipolar coupling frequencies measured with NMR experiments on aligned samples of ^{15}N-labeled proteins. The PISA Wheel plots of chemical shift versus heteronuclear dipolar coupling in the left

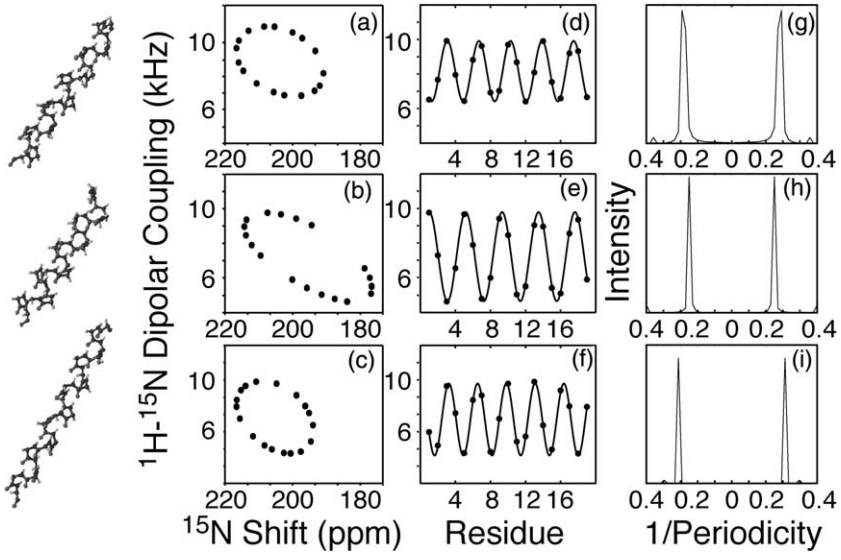

Fig. 1. Simulated data for idealized helices with their average axis of orientation tilted from the z-axis of the aligned frame by 17° for this solid-state NMR data. The second column shows the simulated ^1H–^{15}N PISEMA spectrum for each of these structures. PISA Wheels are shown for an (a) ideal α-helix (b) ideal π-helix, and (c) ideal 3_{10}-helix. Dipolar Waves are plotted by showing only the dipolar coupling as a function of residue number in (d), (e), and (f). The characteristic periodicity is seen as a splitting in the Fourier Transforms shown in (g), (h), and (i). Data for the dipolar couplings was linear predicted by standard methods and the magnitude spectrum is presented.

column (Figs. 1a–c) have characteristic ''wheel-like'' patterns. The corresponding Dipolar Wave plots of dipolar couplings as a function of residue number in the middle column (Figs. 1d–f) exhibit sinusoidal oscillations. The data in the right column (Figs. 1g–i) show that Fourier transformation of the Dipolar Waves gives peaks that are separated by the reciprocal of the periodicity from the center.

The periodicity defines the type of helix, therefore the Dipolar Waves and their Fourier transforms are diagnostic for the type of helix in a protein, which can be difficult to determine based on short-range distances or other properties. For example, while the isotropic chemical shift index (CSI) [51] discriminates between α-helices and β-sheets, the $^{13}C^{\alpha}$, $^{13}C^{\beta}$, $^{1}H^{N}$, and $^{15}N^{H}$ chemical shifts are sensitive to their local environment and are context-dependent [52,53], and as a result are not able to differentiate unambiguously among α, π, and 3_{10} helices. In contrast, because hydrogen bonding and torsion angles are uniform along a helix, variations in structure are expected to have minimal effects on dipolar couplings [54,55]. As a result, the observation of significant deviations from the periodicity associated with one of the three types of helices is highly diagnostic for residues at the ends of helices. Besides their characteristic periods, Dipolar Waves have other features, i.e., amplitudes and average values, that can be used to determine the orientation of a helix in the relevant frame of reference. Further, one side of the sinusoid (manifested as 180° of phase) maps to one face of the α-helix, enabling Dipolar Waves to characterize the rotation (polarity) of the helix about its long axis in the same frame.

Determining the average orientation of the helix axis [θ_{av}, ϕ_{av}] in the alignment frame requires that the influence of the geometry of the helix on θ and ϕ for each N–H bond vector in the polypeptide backbone be taken into account. As shown in Fig. 2a, this can be parameterized as a function of position along the helix in a manner similar to that previously used to describe ^{2}H lineshapes in uniaxially oriented membrane proteins [56] using Eq. (2):

$$D_{NH} = D_a\left\{(3\cos^2\theta - 1) + \frac{3}{2}R(1-\cos^2\theta)\cos 2\phi\right\} \quad (2)$$

with

$$\cos\theta = \cos\theta_{av}\cos\delta - \sin\theta_{av}\sin\delta\cos(\rho-\rho_0)$$

and

$$\phi = \phi_{av} + \sin^{-1}\left(\frac{\sin\delta\sin(\rho-\rho_0)}{\sqrt{1-\cos^2\theta}}\right),$$

where $\delta = 15.8°$ is the angle between the N–H bonds and the helix axis, and D_a and R are the magnitude and rhombicity, respectively, of the tensor that describes the alignment of the protein within the order frame. The

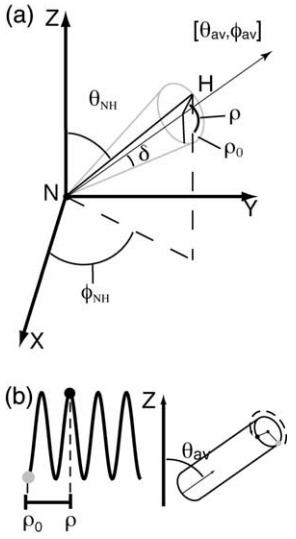

Fig. 2. The geometry of a α-helix determines the values of θ_{NH}, ϕ_{NH} as a function of position (residue number) along the helix because the individual NH bonds are distributed on a cone (a) along the helix axis. θ_{av} and ϕ_{av} give the average helix orientation with δ (= 15.8°) being the angle between the individual HN bonds and this axis. ρ (= $2\pi n/3.6$) is the index of the position along the helix relative to ρ_0. (b) The position of a residue along the sinusoid determines the rotation of a particular residue along that helix axis.

angles θ and ϕ are given as a function of residue number n (with $\rho = 2\pi n/3.6$); θ_{av} and ϕ_{av} are the angles describing the orientation of the helix axis; and ρ_0 describes the rotation (polarity) of the helix in the alignment frame [1]. Examination of this function indicates that, for orientations away from that of the alignment z-axis, this function is well approximated as a simple sinusoidal function with a periodicity of 3.6. The amplitude and average value of the sinusoid vary predictably with the tilt angle of the helix in this frame, as illustrated in Fig. 3 for two different values of R. The average value of the Dipolar Wave for an ideal α-helix (Figs. 3a and c) has a functional dependence on θ_{av}, ϕ_{av} similar to that of a ''virtual'' N–H bond oriented along the helix axis, and has been used as an approximate index of helix orientation in proteins [57,58]. The amplitude of the Dipolar Wave has a more complicated dependence on the orientation of the helix as shown in Figs. 3b and d. The magnitudes of the oscillations are orientation-dependent as well, with the smallest amplitudes for orientations parallel to the alignment z-axis. Because each period of a Dipolar Wave maps to one face of the helix, the value of $\rho - \rho_0$ for a particular residue is indicative of the pitch (rotation) of the individual residue about the helix axis relative to the ρ_0 position as defined in Fig. 2b.

In general, four symmetry-related orientations of a molecular fragment within the order frame are consistent with any single set of measurements. This ambiguity is typically resolved by comparison of datasets obtained from samples with two different order tensors [59,60].

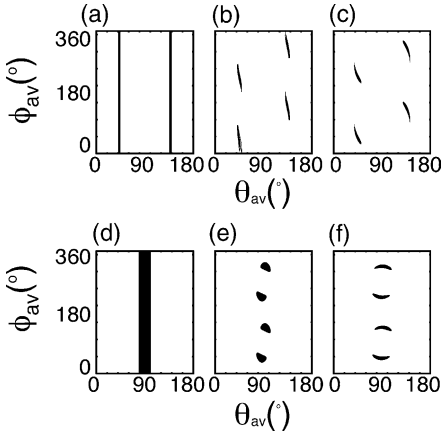

Fig. 4. The expression in Eq. (2) is fitted to data simulated for a α-helix tilted $\theta_{av} = 45°$, $\phi_{av} = 45°$ (a–c) and $\theta_{av} = 85°$, $\phi_{av} = 45°$ (d–f). Simulations are performed for a rhombicity of 0 (a, b), 0.25 (b, e), and 0.60 (c, f). Fits are performed under the assumption that the values of the magnitude and the rhombicity of the alignment are known.

Fig. 4 also shows that there are four orientations of a helix axis consistent with a sinusoid of given average value, amplitude, and phase. The polar angle θ_{av} is determined more accurately than the azimuthal angle ϕ_{av}, although the accuracy of both determinations increases with increasing rhombicity. Alignment with axial symmetry ($R \approx 0$) results in the well-known cone-like degeneracies typically seen in the analysis of dipolar coupling data. The approximate collinearity of N–H bonds in α-helices makes it difficult to determine the axial and rhombic components of the alignment tensor using standard methods [59,61], especially for small or highly helical proteins. In this situation the slight non-collinearity is only consistent with a range of values for D_a. By dividing the values for the Dipolar Wave by the average value across the sinusoid, it is possible to remove the dependence on the magnitude of the alignment (D_a); however, this does not remove the sensitivity to R for higher rhombicity.

4. Kinks and curves in α-helices

Among the advantages of utilizing dipolar couplings to determine molecular structures is that they are purely geometrical in nature, and modest deviations from ideality, as observed in actual protein structures, cause relatively minor but analyzable excursions from the sinusoidal patterns of oscillations in helices. The effects of the most commonly observed deviations from ideal α-helical geometry, classified as "kinks" and "curvature" [62], are illustrated in Fig. 5. The variations of the average values and amplitudes of the sinusoids reflect the differences in torsion angles among individual residues in the helix that result in overall changes in the orientations of the helices. Although the effects of the deviations from

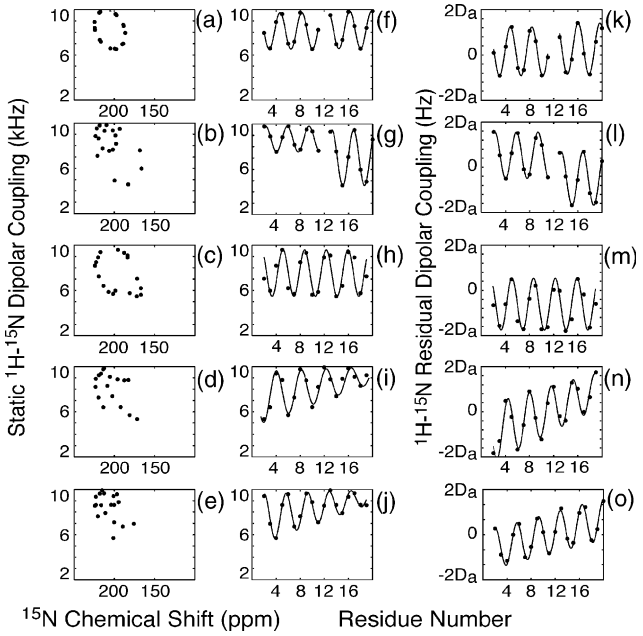

Fig. 5. The effects of common deviations from ideality in α-helices are illustrated. Proline-induced kinks on the order of 30° give a change in amplitude and phase if the θ angle is not strongly affected (a, f, and k), and a large change of phase if this angle is little affected (b, g, and l). In both cases, the disruption of the Dipolar Wave results in a slight alteration of the phase of the sinusoid. A smooth curvature of radius 55 Å also affects the average value and amplitude of the sinusoid more if the θ angle is most changed by the curvature (c, h, and m). This curvature has a more prominent affect if the θ angle is most changed for a large (55 Å radius) or small (65 Å radius) degrees of curvature (d, i, and n) and (e, j, and o), respectively. Simulations are done with the mean axis angle of the helix tilted at 17° for unaveraged dipolar couplings and 45° for residual dipolar couplings relative to the z-axis of the alignment frame. Simulations were done with rhombicity values of 0 and 0.35.

ideal α-helices are orientation-dependent, generally, when the angle θ_{av} for the helix is most affected, the deviation from ideality is most evident. Significantly, the characteristic periodicities of the helices are only slightly affected by their orientations, which contributes to the robustness of the periodicity as an indicator of the length of a helix, regardless of whether it is straight, kinked, or curved. The simulations in Figs. 5a and b show that for a typical kink angle (~30°) the change in average value can be substantial, depending on the value of θ_{av}. As a result, slight changes in the phase of a fitted sinusoid are highly diagnostic for the presence of a kink, although, for a small subset of orientations, the change in average value and amplitude can be minimal.

According to recent analyses, approximately 70% of the α-helices in proteins are defined as smoothly curved, with a mean radius of curvature around 65 Å [63]. Deviations in the fitted sinusoids due to curvature are most obvious in cases where the angle θ_{av} is strongly affected by the change in direction of the helix axis. Figs. 5c and d shows that the pattern of ^{1}H–^{15}N dipolar couplings as

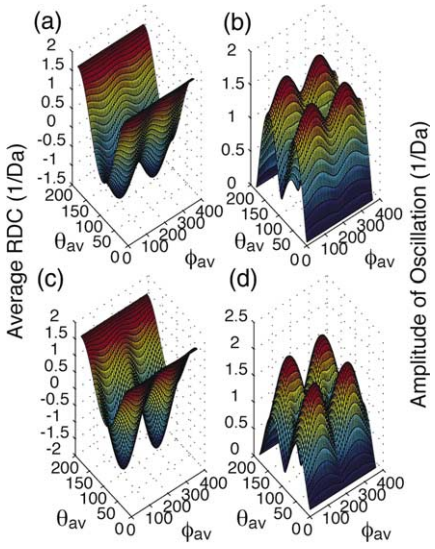

Fig. 3. The average value (a and c) and amplitude (b and d) of the Dipolar Waves vary predictably with the orientation of the helix axis in the oriented frame. Eq. (2) was numerically simulated as a function of helix axis orientation. Rotation of the helix about its axis results in a change of phase of the Dipolar Wave and does not affect the amplitude or average value. Values of the dipolar coupling are normalized so that the magnitude of the coupling would be obtained by multiplying these surfaces by the magnitude of the alignment term D_a. This is shown for values of the rhombicity R of (a and b) 0.25 and (c and d) 0.60.

a function of residue number for an α-helix with radius of curvature 65 Å (average) is unaffected when the curvature does not change the θ_{av} angle describing the average helix axis. And Fig. 5e shows similar effects with an increase in the curvature to a radius of 55 Å. In contrast, the average value and amplitude are altered substantially when the same curvature has the effect of bending the helix axis towards the z-axis of the alignment frame. It is more probable, however, for a helix at a given orientation, that the curvature will indeed change the angle θ_{av} along the helix. Identification of the faces of the helix on the inside and outside of the curve can be made based on the residues that map to each 180° of phase of the sinusoid. Variations in the amplitudes and average values of dipolar couplings are sufficient to describe the effects of curvature on the appearance of Dipolar Waves.

5. Dipolar Waves in experimental data

The helical residues in a representative sample of soluble proteins exhibit the characteristic 3.6 residue per turn periodicity in the oscillations of their ^1H–^{15}N RDCs, as shown in Fig. 6. Moreover, differences in the orientations of helices within the same polypeptide are clearly reflected in the differences of amplitude and average value of the corresponding Dipolar Waves. While the periodicity of 3.6 residues per turn is evident upon visual inspection in most cases, uncertainties can arise when there are missing or incorrectly assigned measurements. Indeed, an otherwise well-fit sinusoid is an extremely useful way to detect incorrect resonance assignments, since misassigned data points are typically off the wave pattern defined by the other points. All of the Dipolar Waves shown in the figure were fit automatically using the four-residue sliding window function. The non-helical segments of the proteins are equally obvious by inspection because of their lack of periodicity.

It is straightforward to apply an algorithm that fits the experimental data to a sinusoid with a specific periodicity, and then separately assesses the error associated with making this assumption. The average error per measurement is given by Eq. (3), independent of any estimate for the magnitude and rhombicity of the alignment:

$$\chi = \frac{1}{N}\sum_{N} |D_{obs} - D_{ideal}|. \quad (3)$$

This can be used initially to identify those regions in a polypeptide that have a structural feature with a periodicity of 3.6 residues. In this case D_{ideal} can be simply approximated as a function of residue number (n) by $[A\sin(\rho - f_0) + K]$ where A is the difference between the largest and smallest measurements in this window, ρ as defined previously, and K is the average value of the sinusoid in that window. A, K, and f_0 are floating parameters optimized using a standard nonlinear least squares fitting routine. We have found that a window containing between four and six residues ($N = 4$–6) detects the intrinsic periodicity of the oscillations of the ^1H–^{15}N dipolar couplings with little sensitivity to imperfections of the helices or errors in the measurements. Typical χ scores for α-helices fitted in this way are significantly smaller than the experimental error for most helices, while helices with substantial imperfections, non-idealities, or experimental errors give values slightly larger than the experimental error for each point. In contrast, non-helical regions have values that are 5–10 times larger than the experimental error of the measurements. The plots in Fig. 6 show that the residues identified as α-helical based solely on periodicity are in excellent agreement with findings based on the standard parameters of NOEs, J-couplings, hydrogen bonds, and CSI. In all cases, χ is less than the experimental errors for the datasets for all helices with four or more residues. The inclusion of measurements from any residues with non-helical conformations results in a large increase in the score due to a perturbation in the characteristic periodicity. While it is possible to occasionally satisfy an ideal sinusoidal dependence for a given window of four to six residues (e.g., four zeroes in a row), this rarely occurs for consecutive windows. For this reason it is

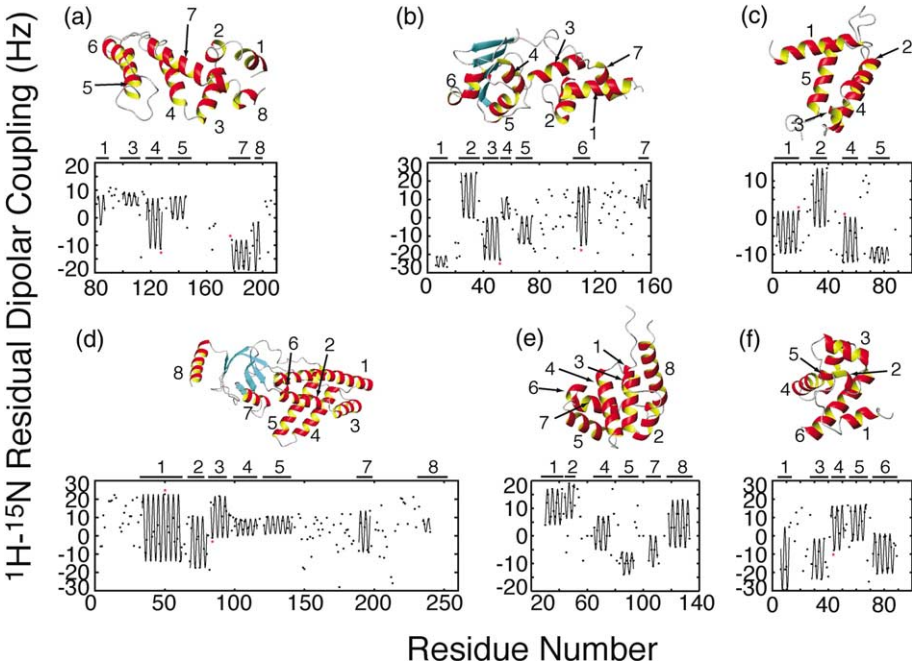

Fig. 6. Plots of experimentally measured ^{1}H–^{15}N RDCs as a function of residue number. Best fitting sinusoids are superimposed on the experimental data to demonstrate the periodicity. Experimental data was used in the determination of the structures for proteins (a) 1CMZ [33], (b) 1C06 [34], (c) 1B4C [35], (d) 3EZA [36], (e) 1JWE [37], and (f) 2EZX [38]. Horizontal bars denote the positions of the α-helices according to the PDB classifications. All helical regions score less than 0.4 Hz RMSD to the ideal sinusoid. Possible errors are denumerated by an asterisk based on significant deviations from the sinusoid, inconsistent with their known helicity. In some cases this is mentioned in the restraint files deposited at BioMagRes.

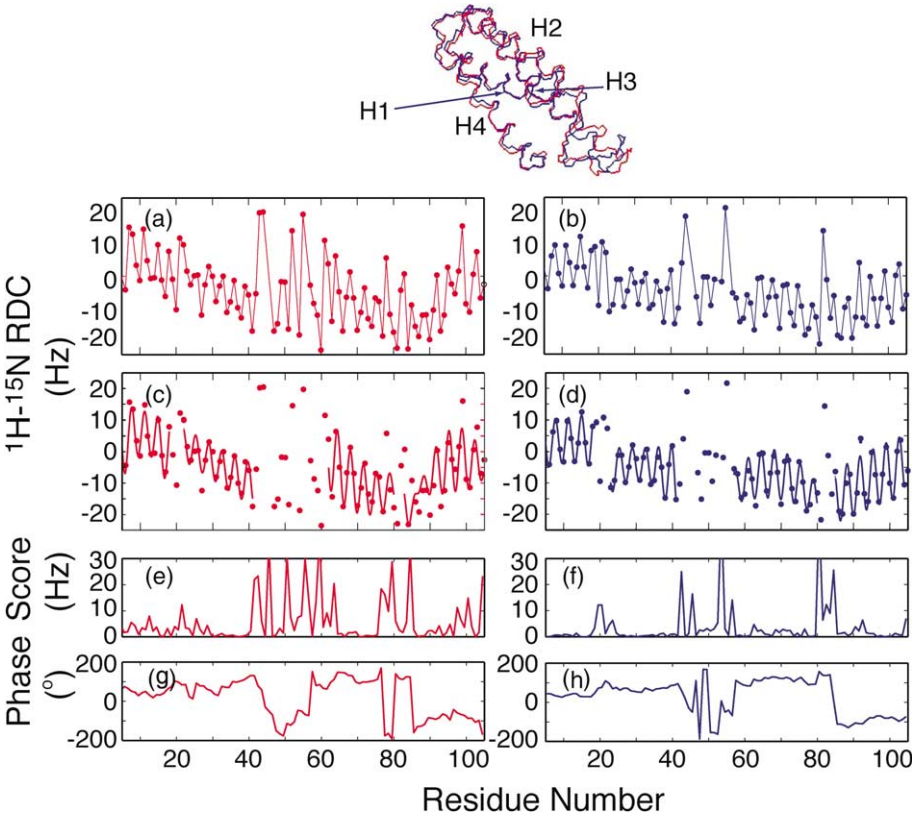

Fig. 7. Simulated ^{1}H–^{15}N residual dipolar couplings ($D_a = 15$ Hz and $R = 0.6$) for cytochrome b_{652} for two different structures at the alignment shown. (a, b) Data for the mean NMR structure are shown in red and the 1.4 Å resolution crystal structure are shown in blue. (c, d) The best fitting Dipolar Waves are shown superimposed on data for the helical regions where R_{dip} is less than 25%. (e, f) The score to a sinusoid of periodicity 3.6 is shown for each 4-residue window. Regions with low scores are considered to be helical. (g, h) The absolute phase is also a monitor of the lengths of the helices.

useful to examine not only the sinusoid itself but also the absolute phases.

Because the deviation from ideality is sensitive to the magnitude and rhombicity of the alignment tensor, a more objective measure of the agreement between the experimental data and this ideal sinusoidal dependence is given by calculated values for R_{dip} [64] (ranging from 0 to 1, where 0 reflects perfect agreement and 1 reflects lack of agreement).

$$R_{\mathrm{dip}}\sqrt{\frac{5\langle(D_{\mathrm{obs}}-D_{\mathrm{ideal}})^2\rangle}{2D_{\mathrm{a}}^2(4+3R^2)}}. \tag{4}$$

For the magnitudes of alignment seen in these examples, these errors correspond to values of R_{dip} between 5 and 15%. Remarkably, the fit of Dipolar Waves to dipolar coupling datasets simulated from high-resolution (RMSD < 2 Å) structures are on-average 5–10% higher. This is most likely due to the high sensitivity of dipolar couplings to small irregularities, or any ''structural noise'' introduced by the structure calculation process [65]. Generally, the inclusion of dipolar couplings in structure calculation and refinement protocols improves the geometry of helical regions, making them more ideal [66,67]. Values for R_{dip} less than 25% typically provide satisfactory fits to the experimental data. Based on simulations of a large number of α-helices with deviations from ideal geometry, we find that an R_{dip} of 25% corresponds to a backbone RMSD of 1.5 Å from an ideal helix, and an R_{dip} of 10% corresponds to a backbone RMSD of 0.7 Å. The R_{dip} values for fits of sinusoids to experimental dipolar couplings indicate that typical α-helices differ from ideal α-helices with RMSDs less than 1.0 Å.

In general, the values for R_{dip} can be reduced to less than 5% for experimental datasets and less than 10% for simulated datasets if the average value and amplitude of the sinusoid are allowed to vary quadratically along the helix. However, it can be difficult to interpret these findings because the number of fitting parameters may exceed the number of data points. As an example, residual dipolar couplings were simulated for the three-dimensional structure of cytochrome b_{562}, a protein with 81 of its 106 residues in four α-helices using a typical alignment magnitude (Figs. 7a and b). Because the NMR structure [39] contains helices that are more distorted than the X-ray diffraction structure [40] it is useful to compare the datasets simulated for the same alignment. In both cases, the helices can be clearly identified based on their characteristic periodicity, as shown in Figs. 7e and f. The values of R_{dip} for the fits of these helices using an ideal sinusoid are larger than 25% for the NMR structure and less than 25% for the 1.4 Å resolution crystal structure. Significantly, incorporating amplitude and average value variations along the helices reduces the values of R_{dip} less than 25% for three of the four helices in the NMR structure and less than 10% for the crystal structure. This demonstrates that Dipolar Waves are sensitive to the deformations and curvatures of helices found in experimentally determined protein structures, although such deviations are rare in high quality structures, whether determined by NMR spectroscopy or X-ray crystallography. Even in this example, the deviations may reflect the structure calculation and refinement process rather than the protein structure itself.

6. Determination of helix orientations

If the magnitude and rhombicity of the alignment tensor (D_{a} and R) can be determined reliably from measurements of the ^{1}H–^{15}N RDCs, accurate determinations of the orientations of these helices in the order frame can be made. Using constant values for the magnitude of this tensor, Eq. (2) can be fitted to the sinusoid that describes the periodicity of oscillations of the dipolar couplings. This results in best-fitted values of θ_{av}, ϕ_{av}, and ρ_0; θ_{av} and ϕ_{av} give the orientation of the helix in the orientation frame and ρ_0 is used to determine the rotation of a residue relative to the helix axis. As an example, Fig. 8 shows the overlap of a simple sinusoid with the experimentally measured ^{1}H–^{15}N RDCs for two different helices taken from the examples shown in Fig. 6. Not only is a simple sinusoid consistent with the experimental measurements, but also Eq. (2) can be fitted to the data to obtain the average tilt of the helix in the alignment frame as well as ρ_0, the absolute rotation of the helix. The rotation of a particular residue about the long axis of the helix can be determined from the value of $\omega_n = (n \times 360°)/3.6 - \rho_0$ (in degrees) because ρ_0 is defined as shown in Fig. 2.

In practice, the fitting of Dipolar Waves yields four possible solutions for the orientations of helices found in proteins; but in cases where data for two different order frames are available these ambiguities can be resolved, yielding the actual relative orientations of the helices. As an example, the structure of one of the subunits of S100B [35] is shown in Fig. 9a along the axes of the alignment tensor as determined by the program MODULE. For each helix there are four solutions consistent with the experimental data as depicted in Figs. 9c–f, for each helix one of which is correct. If another dataset had been available, the correct orientation could have been selected and used to construct a model as shown in Fig. 9b. Fig. 10 shows that the θ_{av} and ϕ_{av} angles for the helices in all of these examples can be fitted to obtain the actual angles of the helices in the oriented frame with a correlation coefficient of 0.98 in both cases. The starting values for the fitting algorithm are chosen so that the convergence is in the proper quadrant. Nonetheless, the average error in the determination of the angle θ_{av} is 4°

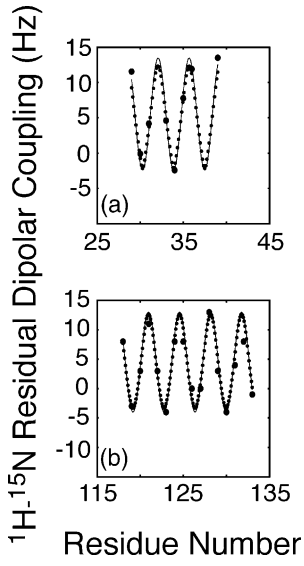

Fig. 8. Experimentally measured values of the ^{1}H–^{15}N RDCs for helix number 2 in rat Apo-S100B28 and helix number 8 in DnaB helicase as a function of residue number. The regions identified as helical from the score can be correlated to both a simple sinusoid and the expression given in Eq. (2) {dotted line} that gives the average tilt angles (θ_{av} and ϕ_{av}) and ρ_0 in the oriented frame. The ideal sinusoid most consistent with these measurements overlays with a χ of 0.3 Hz and this agrees quite well with the best-fitted sinusoid obtained from Eq. (2). Values of D_a (R) were 7.75 Hz (0.54) and 9.14 Hz (0.25) for Apo-S100B and DnaB helicase, respectively. (a) For helix 2 of Apo-S100B the fit gives values of 145° for θ_{av} and 88° for ϕ_{av}, $\rho_0 = -19°$. From the position of ρ_0, the rotation of residue Glu 31 can be determined to be rotated $\omega_{31} = (31 \times 360°)/3.6 - (-19°) = 239°$ relative to ρ_0 as defined in Fig. 2. (b) For DnaB helicase helix 8, values for $\theta_{av} = 138°$ and $\phi_{av} = 260°$ are determined with $\rho_0 = 124°$. Residue Asp 123 is then rotated $\omega_{123} = (123 \times 360°) - 124° = 296°$ as shown.

and the average error in ϕ_{av} is 9°, consistent with the fact that the ϕ_{av} angle is less well determined. The relative rotations of the helices are also correct to within 4°.

7. Conclusions

The anisotropy of nuclear spin interactions results in a mapping of protein structure onto the resonance frequencies and splittings measured in NMR experiments performed on aligned samples. Dipolar Waves [1], as an extension of PISA Wheels [47,48], provide a straightforward example of mapping of the structural periodicity of helices onto NMR data. In the case of Dipolar Waves, the mapping takes the form of sinusoidal oscillations of dipolar couplings as a function of residue number. The analysis of the fitting of experimental data fit to sinusoids provides a remarkable amount of structural information. Further, Dipolar Waves have the advantage of providing a way to analyze the results from solution NMR and solid-state NMR studies of proteins in a consistent and directly comparable manner.

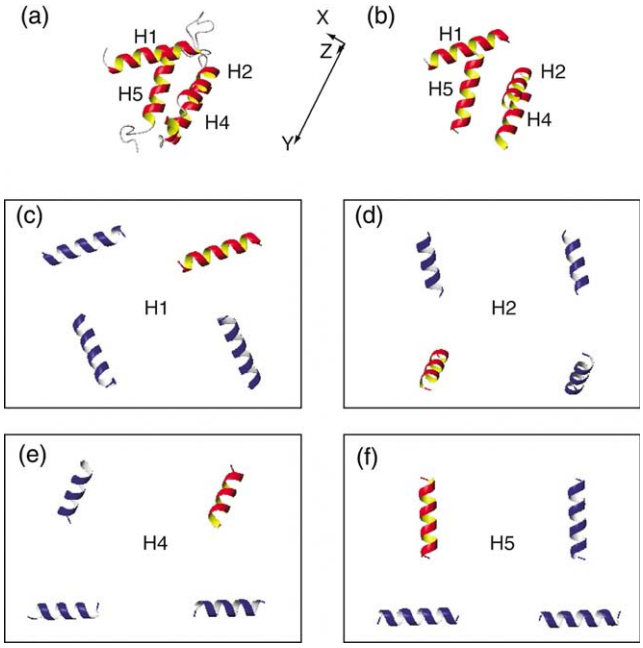

Fig. 9. (a) The NMR structure of subunit 1 of Apo-S100B is shown with the axes of the tensor that describes the alignment as determined by MODULE. The four possible orientations consistent with the measurements for each helix are shown in (c), (d), (g), and (f) with the correct orientation colored red as shown in (b).

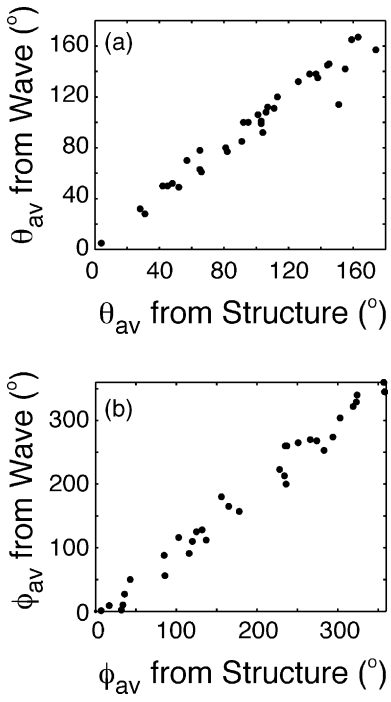

Fig. 10. Plots showing the correlation between the actual values of the tilt angles of helices in the high-resolution structures and the values determined from Dipolar Waves. The values of θ_{av} (a) correlate better than the values of ϕ_{av} (b). The starting values of the fitting procedure were chosen so that the fit converges to the solution in the proper quadrant.

Dipolar Waves have a particular role as a bridge between some of the data obtained in the early stages of NMR studies of proteins and the determination of the complete three-dimensional structures. They have the important advantage of being applicable to incomplete data sets since it is possible to fit sinusoids to data with some missing or misassigned values. Indeed, periodicity is such a strict requirement that individual dipolar couplings that do not fit to an otherwise well-fit sinusoid are almost always misassigned, or measured incorrectly due to overlap, broadening, or other experimental problems.

As a first step in structure determination, the Dipolar Wave analysis is especially valuable when the protein is highly helical. Limitations exist for a small subset of helix orientations where oscillations are not observed. In these cases, the measurement of spectral parameters associated with other interactions, such as $^{13}C^{\alpha}$–$^{1}H^{\alpha}$ residual dipolar couplings and ^{13}C chemical shifts can be used to supplement the identification, positioning, and removal of orientational ambiguity in the calculations. Large numbers of missing measurements complicate the analysis. This can result from resonance overlap or the flexibility and dynamics inherent to some proteins, as can be seen, for example, in the mitochondrial protein p8 [68]. In such cases, short-range NOEs and the CSI may be used to supplement the dipolar coupling measurements in a manner that explicitly accounts for the dynamics of the protein.

Dipolar Waves can be combined with more conventional structure determination procedures in order to make use of covalent geometry and standard energy minimization protocols. One such approach, proposed by Prestegard et al. [69], uses a pseudopotential for the packing density of the helices in combination with short-range NOE information to define the positions of the α-helices. Dipolar Waves can be supplemented with orientational information for regions in between these secondary structure elements, as well as an experimental determination of the contribution of local dynamics to the measured couplings and shifts. This information, in combination with the covalent geometry of the linker regions, enables the distances between rigid subunits of a protein to be estimated with moderate accuracy, replacing "intermolecular" distances. A strong potential enables this information to serve as strong constraints on the orientations of helices [70] in the structure of the protein.

Dipolar Waves are particularly useful in cases where higher levels of experimental data are difficult to obtain because of sample limitations, which is frequently the case for membrane proteins. Or, when speed is of the essence in high throughput applications where the fold of the protein can be determined from the relative orientations and other properties of α-helices. Moreover, Dipolar Waves can provide a direct window on conformational changes of proteins.

Acknowledgments

We thank D.H. Jones, S. Lee, F. Marassi, A. Nevzorov, and G. Veglia for helpful discussions. This research was supported by Grants R37GM24266, PO1GM64676, RO1GM29754, and PO1GM56538 from the National Institutes of Health. The research benefited from the Biomedical Technology Resources for Solid-State NMR of Proteins supported by Grant P41RR09789.

References

[1] M.F. Mesleh, G. Veglia, T.M. DeSilva, F.M. Marassi, S.J. Opella, Dipolar waves as NMR maps of protein structure, J. Am. Chem. Soc. 124 (2002) 4206–4207.
[2] S.J. Opella, A. Nevzorov, M.F. Mesleh, F.M. Marassi, Structure determination of membrane proteins by NMR spectroscopy, Biochem. Cell Biol. 80 (2002) 597–604.
[3] F.M. Marassi, A simple approach to membrane protein secondary structure and topology based on NMR spectroscopy, Biophys. J. 80 (2001) 994–1003.
[4] C. Altenbach, T. Marti, H.G. Khorana, W.J. Hubbell, Transmembrane protein-structure—Spin labeling of Bacteriorhodopsin mutants, Science 248 (1990) 1088–1092.
[5] K.A. Bolin, P. Hanson, S.J. Wright, G.L. Millhauser, An NMR investigation of the conformational effect of nitroxide spin labels on Ala-rich helical peptides, J. Magn. Reson. 131 (1998) 248–253.
[6] M.D. Rabenstein, Y.K. Shin, Determination of the distance between 2 spin labels attached to a macromolecule, Proc. Natl. Acad. Sci. USA 92 (1995) 8239–8243.
[7] A. Pardi, G. Wagner, K. Wuthrich, Protein conformation and proton NMR chemical-shifts, Eur. J. Biochem. 137 (1983) 445–454.
[8] L. Szilagyi, O. Jardetzky, α-Proton chemical-shifts and secondary structure in proteins, J. Magn. Reson. 83 (1989) 441–449.
[9] M.P. Williamson, Secondary-structure dependent chemical-shifts in proteins, Biopolymers 29 (1990) 1428–1431.
[10] A.C. De Dios, J.G. Pearson, E. Oldfield, Secondary and tertiary structural effects on protein NMR chemical-shifts—an ab initio approach, Science 260 (1993) 1491–1496.
[11] I.D. Kuntz, P.A. Kosen, E.C. Craig, Amide chemical-shifts in many helices in peptides and proteins are periodic, J. Am. Chem. Soc. 113 (1991) 1406–1408.
[12] F.J. Blanco, J. Herranz, C. Gonzalez, M.A. Jimenez, M. Rico, J. Santoro, J.L. Nieto, NMR chemical-shifts—a tool to characterize distortions of peptide and protein helices, J. Am. Chem. Soc. 114 (1992) 9676–9677.
[13] J.A. Whiles, R. Brasseur, K.J. Glover, G. Melacini, E.A. Komives, R.R. Vold, Orientation and effects of mastoparan X on phospholipid bicelles, Biophys. J. 80 (2001) 280–293.
[14] S.J. Opella, P.L. Stewart, K.G. Valentine, Protein-structure by solid-state NMR-spectroscopy, Q. Rev. Biophys. 19 (1987) 7–49.
[15] S. Pausak, A. Pines, J.S. Waugh, Carbon-13 chemical shielding tensors in single-crystal durene, J. Chem. Phys. 59 (1973) 599–612.
[16] S.J. Opella, J.S. Waugh, 2-Dimensional C-13 NMR of highly oriented polyethylene, J. Chem. Phys. 66 (1977) 4919–4924.

[17] A. Bax, G. Kontaxis, N. Tjandra, Dipolar couplings in macromolecular structure determination, Meth. Enzymol. 339 (2001) 127–174.
[18] A. Saupe, Recent results in the field of liquid crystals, Angew. Chem. Intl. Ed. 7 (1968) 97–112.
[19] A.A. Bothner-By, in: D.M. Grant, R.K. Harris (Eds.), Encyclopedia of Nuclear Magnetic Resonance, Wiley, Chichester, 1996, pp. 2932–2938.
[20] S.J. Opella, NMR and membrane proteins, Nat. Struct. Biol. 4 (1997) 845–848.
[21] F.M. Marassi, A. Ramamoorthy, S.J. Opella, Complete resolution of the solid-state NMR spectrum of a uniformly ^{15}N-labeled membrane protein in phospholipid bilayers, Proc. Natl. Acad. Sci. USA 94 (1997) 8551–8556.
[22] C. Ma, S.J. Opella, Lanthanide ions bind specifically to an added "EF-hand" and orient a membrane protein in micelles for solution NMR spectroscopy, J. Magn. Reson. 146 (2000) 381–384.
[23] G. Veglia, S.J. Opella, Lanthanide ion binding to adventitious sites aligns membrane proteins in micelles for solution NMR spectroscopy, J. Am. Chem. Soc. 122 (2000) 11733–11734.
[24] H.J. Sass, G. Musco, S.J. Stahl, P.T. Wingfield, S. Grzesiek, Solution NMR of proteins within polyacrylamide gels: diffusional properties and residual alignment by mechanical stress or embedding of oriented purple membranes, J. Biomol. NMR 18 (2000) 303–309.
[25] Y. Ishii, M.A. Markus, R. Tycko, Controlling residual dipolar couplings in high-resolution NMR of proteins by strain induced alignment in a gel, J. Biomol. NMR 21 (2001) 141–151.
[26] J.J. Chou, S. Gaemers, B. Howder, J.M. Louis, A. Bax, A simple apparatus for generating stretched polyacrylamide gels, yielding uniform alignment of proteins and detergent micelles, J. Biomol. NMR 21 (2001) 377–382.
[27] http://www-lecb.ncifcrf.gov/~kumarsan/HELANAL/helanal.html.
[28] T.E. Creighton, Proteins: Structures and Molecular Properties, Freeman, New York, 1993.
[29] N.E. Zhou, B.Y. Zhu, B.D. Sykes, R.S. Hodges, Relationship between amide proton chemical-shifts and hydrogen-bonding in amphipathic α-helical peptides, J. Am. Chem. Soc. 114 (1992) 4320–4326.
[30] M.F. Mesleh, K.G. Valentine, S.J. Opella, J.M. Louis, A.M. Gronenborn, Myristoylation as a general method for immobilization and alignment of soluble proteins for solid-state NMR structural studies, J. Biomol. NMR 25 (2003) 55–61.
[31] http://www.bmrb.wisc.edu/ B.R. Seavey, E.A. Farr, W.M. Westler, J.L. Markley, A relational database for sequence-specific NMR data, J. Biomol. NMR 1 (1) (1991) 217–236.
[32] http://www.rcsb.org/pdb/ H.M. Berman, J. Westbrook, Z. Feng, G. Gilliland, T.N. Bhat, H. Weissig, I.N. Shindyalov, P.E. Bourne, The protein data bank, Nucleic Acid Res. 28 (2000) 235–242.
[33] E. de Alba, L. De Vries, M.G. Farquhar, N. Tjandra, Solution structure of human GAIP (G^{α} interacting protein): a regulator of G protein signaling, J. Mol. Biol. 291 (1999) 927–939.
[34] M.A. Markus, R.B. Gerstner, R.B. Draper, D.A. Torchia, The solution structure of ribosomal protein S4 δ 41 reveals two subdomains and a positively charged surface that may interact with RNA, EMBO J. 17 (1998) 4559–4571.
[35] A.C. Drohat, D.M. Baldisseri, R.R. Rustandi, D.J. Weber, Solution structure of calcium-bound rat S100B(ββ) as determined by nuclear magnetic resonance spectroscopy, Biochemistry 37 (1998) 2729–2740.
[36] D.S. Garrett, Y.J. Seok, A. Peterkofsky, A.M. Gronenborn, G.M. Clore, Solution structure of the 40,000 M-r phosphoryl transfer complex between the N-terminal domain of enzyme I and Hpr, Nat. Struct. Biol. 6 (1999) 166–173.
[37] J. Weigelt, S.E. Brown, C.S. Miles, N.E. Dixon, G. Otting, NMR structure of the N-terminal domain of *E. coli* DNAb helicase: implications for structure rearrangements in the helicase hexamer, Struct. Fold. Des. 7 (1999) 681–690.
[38] M. Cai, Y. Huang, R. Zheng, S.Q. Wei, R. Ghirlando, M.S. Lee, R. Craigie, A.M. Gronenborn, G.M. Clore, Solution structure of the cellular factor BAF responsible for protecting retroviral DNA from autointegration, Nat. Struct. Biol. 5 (1998) 903–909.
[39] F. Arnesano, L. Banci, I. Bertini, J. Faraone-Mennella, A. Rosato, P.D. Barker, A.R. Fersht, The solution structure of oxidized *Escherichia coli* cytochrome b_{562}, Biochemistry 38 (1999) 8657–8670.
[40] F. Lederer, A. Glatigny, P.H. Bethge, H.D. Bellamy, F.S. Mathews, Improvement of the 2.5 Å resolution model of cytochrome-b_{562} by redetermining the primary structure and using molecular graphics, J. Mol. Biol. 148 (1981) 427–448.
[41] G.M. Clore, A.M. Gronenborn, A. Bax, A robust method for determining the magnitude of the fully asymmetric alignment tensor of oriented macromolecules in the absence of structural information, J. Magn. Reson. 133 (1998) 216–221.
[42] P. Dosset, J.C. Hus, D. Marion, M. Blackledge, A novel interactive tool for rigid-body modeling of multi-domain macromolecules using residual dipolar couplings, J. Biomol. NMR 20 (2001) 223–231.
[43] R. Koradi, M. Billeter, K. Wuthrich, MOLMOL: A program for display and analysis of macromolecular structures, J. Mol. Graph. 14 (1996) 51–55.
[44] N.A. Christopher, R. Swanson, T.O. Baldwin, Algorithms for finding the axis of a helix: fast rotational and parametric least-squares methods, Comp. Chem. 20 (1996) 339–345.
[45] T. Vosegaard, N. Nielsen, Towards high-resolution solid-state NMR on large uniformly ^{15}N and [^{13}C, ^{15}N]-labeled membrane proteins in oriented lipid bilayers, J. Biomol. NMR 22 (2002) 225–247.
[46] S. Kim, T.A. Cross, Uniformity, ideality, and hydrogen bonds in transmembrane α-helices, Biophys. J. 83 (2002) 2084–2095.
[47] F.M. Marassi, S.J. Opella, A solid-state NMR index of helical membrane protein structure and topology, J. Magn. Reson. 144 (2000) 150–155.
[48] J. Wang, J. Denny, C. Tian, S. Kim, Y. Mo, F. Kovacs, Z. Song, K. Nishimura, Z. Gan, R. Fu, J.R. Quine, T.A. Cross, Imaging membrane protein helical wheels, J. Magn. Reson. 144 (2000) 162–167.
[49] F.M. Marassi, S.J. Opella, Using Pisa pies to resolve ambiguities in angular constraints from PISEMA spectra of aligned proteins, J. Biomol. NMR 23 (2002) 239–242.
[50] D. Eisenberg, R.M. Weiss, T.C. Terwilliger, The hydrophobic moment detects periodicity in protein hydrophobicity, Proc. Natl. Acad. Sci. USA 81 (1984) 140–144.
[51] D.S. Wishart, B.D. Sykes, The ^{13}C chemical shift index: a simple method for the identification of protein secondary structure using ^{13}C chemical shift data, J. Biomol. NMR 4 (1994) 171–180.
[52] S. Schwarzinger, G.J.A. Kroon, T.R. Foss, J. Chung, P.E. Wright, H.J. Dyson, Sequence-dependent correction of random coil NMR chemical shifts, J. Am. Chem. Soc. 123 (2001) 2970–2978.
[53] G. Cornilescu, A. Bax, Measurement of proton, nitrogen, and carbonyl chemical shielding anisotropies in a protein dissolved in a dilute liquid crystalline phase, J. Am. Chem. Soc. 122 (2000) 10143–10154.
[54] D.A. Case, Calculations of NMR dipolar coupling strengths in model peptides, J. Biomol. NMR 15 (1999) 95–102.
[55] N. Tjandra, A. Bax, Solution NMR measurement of amide proton chemical shift anisotropy in ^{15}N-enriched proteins, correlation with hydrogen bond length, J. Am. Chem. Soc. 119 (1997) 8076–8082.
[56] A.S. Ulrich, A. Watts, ^{2}H NMR lineshapes of immobilized uniaxially oriented membrane-proteins, Solid State Nucl. Magn. Reson. 2 (1993) 21–36.

[57] V. Tsui, L.M. Zhu, T.H. Huang, P.E. Wright, D.A. Case, Assessment of zinc finger orientations by residual dipolar coupling constants, J. Biomol. NMR 16 (2000) 9–21.
[58] B.E. Ramirez, O.N. Voloshin, R.D. Camerini-Otero, A. Bax, Solution structure of DinI provides insight into its mode of RecA inactivation, Prot. Sci. 9 (2000) 2161–2169.
[59] J.A. Losonczi, M. Andrec, M.W.F. Fischer, J.H. Prestegard, Order matrix analysis of residual dipolar couplings using singular value decomposition, J. Magn. Reson. 138 (1999) 334–342.
[60] H.M. Al-Hashimi, H. Valafar, M. Terrell, E.R. Zartler, M.K. Eidsness, J.H. Prestegard, Variation of molecular alignment as a means of resolving orientational ambiguities in protein structures from dipolar couplings, J. Magn. Reson. 143 (2000) 402–406.
[61] M.W.F. Fischer, J.A. Losonczi, J.L. Weaver, J.H. Prestegard, Domain orientation and dynamics in multidomain proteins from residual dipolar couplings, Biochemistry 38 (1999) 9013–9022.
[62] D.J. Barlow, J.M. Thornton, Helix geometry in proteins, J. Mol. Biol. 201 (1988) 601–619.
[63] S. Kumar, M. Bansal, Structural and sequence characteristics in long α-helices of globular proteins, Biophys. J. 71 (1998) 1574–1586.
[64] G.M. Clore, D.S. Garrett, R-factor, free R, and complete cross-validation for dipolar coupling refinement of NMR structures, J. Am. Chem. Soc. 121 (1999) 9008–9012.
[65] M. Zweckstetter, A. Bax, Evaluation of uncertainty in alignment tensors obtained from dipolar couplings, J. Biomol. NMR 23 (2002) 127–137.
[66] N. Tjandra, J.G. Omichinski, A.M. Gronenborn, G.M. Clore, A. Bax, Use of dipolar ^{1}H–^{15}N and ^{1}H–13C couplings in the structure determination of magnetically oriented macromolecules in solution, Nat. Struct. Biol. 4 (1997) 732–738.
[67] J.F. Wang, S. Kim, F. Kovacs, T.A. Cross, Structure of the transmembrane region of the M2 protein H^{+} channel, Prot. Sci. 10 (2001) 2241–2250.
[68] H. Demene, T. Ducat, P. Barthe, M.A. Delsuc, C. Roumestand, Structure refinement of flexible proteins using dipolar couplings: application to the protein p8MTCP1, J. Biomol. NMR 22 (2002) 47–56.
[69] J.H. Prestegard, J.R. Tolman, A. Al-Hashimi, M. Andrec, in: N. Rama Krishna, L.O. Berliner (Eds.), Biological Magnetic Resonance: Structure Computation and Dynamics in Protein NMR, Kluwer, Plenum Press, 1999.
[70] G.M. Clore, C.A. Bewley, Using conjoined rigid body/torsion angle simulated annealing to determine the relative orientation of covalently linked protein domains from dipolar couplings, J. Magn. Reson. 154 (2002) 329–335.